YALE JOURNAL OF BIOLOGY AND MEDICINE 92 (2019), pp.385-396.

ORIGINAL CONTRIBUTION

YALE JOURNAL OF BIOLOGY AND MEDICINE
YJBM
CELEBRATING 90 YEARS 1928–2018

The Short N-Terminal Repeats of Transcription Termination Factor 1 Contain Semi-Redundant Nucleolar Localization Signals and P19-ARF Tumor Suppressor Binding Sites

Joël Boutin[a,b,c], Frédéric Lessard[a,b,d], Michel G. Tremblay[a], and Tom Moss[a,b,*]

[a]*Laboratory of Growth and Development, St-Patrick Research Group in Basic Oncology, Cancer Division of the Quebec University Hospital Research Centre (Axe Cancer, CR-CHU de Québec), Quebec, QC, Canada;* [b]*Department of Molecular Biology, Medical Biochemistry and Pathology, Faculty of Medicine, Université Laval, Quebec, QC, Canada;* [c]*Endocrinology and Nephrology Division of the Quebec University Hospital Research Centre (Axe endocrinologie et néphrologie, CR-CHU de Québec), Quebec, QC, Canada;* [d]*Department of Biochemistry and Molecular Medicine, Université de Montréal, Montréal, QC, Canada*

The p14/p19^{ARF} (ARF†) tumor suppressor provides an important link in the activation of p53 (TP53) by inhibiting its targeted degradation via the E3 ligases MDM2/HDM2. However, ARF also limits tumor growth by directly inhibiting ribosomal RNA synthesis and processing. Initial studies of the ARF tumor suppressor were compounded by overlap between the INK4A and ARF genes encoded by the CDKN2A locus, but mouse models of pure ARF-loss and its inactivation in human cancers identified it as a distinct tumor suppressor even in the absence of p53. We previously demonstrated that both human and mouse ARF interact with Transcription Termination Factor 1 (TTF1, TTF-I), an essential factor implicated in transcription termination and silencing of the ribosomal RNA genes. Accumulation of ARF upon oncogenic stress was shown to inhibit ribosomal RNA synthesis by depleting nucleolar TTF1. Here we have mapped the functional nucleolar localization sequences (NoLS) of mouse TTF1 and the sequences responsible for interaction with ARF. We find that both sequences lie within the 25 amino acid N-terminal repeats of TTF1. Nucleolar localization depends on semi-redundant lysine-arginine motifs in each repeat and to a minor extent on binding to target DNA sequences by the Myb homology domain of TTF1. While nucleolar localization of TTF1 predominantly correlates with its interaction with ARF, NoLS activity and ARF binding are mediated by distinct sequences within each N-terminal repeat. The data suggest that the N-terminal repeats of mouse TTF1, and by analogy those of human TTF1, cooperate to mediate both nucleolar localization and ARF binding.

*To whom all correspondence should be addressed: Tom Moss, Department of Molecular Biology, Medical Biochemistry and Pathology, Faculty of Medicine, Université Laval, Quebec, QC, Canada; Tel: 418-525-4444 ext. 15549; Fax: 418-691-5439; Email: tom.moss@crhdq.ulaval.ca.

†Abbreviations: ARF, Alternative Reading Frame of CDKN2A; mARF, mouse p19^{ARF}; hARF, human p14^{ARF}; TTF1, Transcription Termination Factor 1; RPI/PolI/POLR1, RNA polymerase 1; rRNA, ribosomal RNA; rDNA, ribosomal RNA genes; IP, Immunoprecipitation; a.a., amino acid.

Keywords: p19/p14ARF, tumor suppressor, ribosome biogenesis, RNA polymerase I, Transcription Termination Factor 1, Nucleolar localization sequence

Author Contributions: JB and FL performed the major experimental manipulations. MGT provided technical support. TM provided guidance and wrote manuscript.

INTRODUCTION

A general property of tumor suppressors is their ability, either directly or indirectly, to repress protein synthesis and arrest the cell cycle [1,2]. This property is at least in part mediated by the regulation of ribosome biogenesis [3-6]. Indeed, the targeted repression of ribosome biogenesis resembles many aspects of tumor suppression, including arrest of the cell cycle and the induction of apoptosis [7,8]. Several agents used in chemotherapy have also been shown to suppress ribosome biogenesis, in some cases acting directly on key RNA Polymerase I (RPI/PolI/PolR1) transcription factors to repress the synthesis of ribosomal RNA (rRNA). Examples are Cisplatin that targets the essential RPI factor UBF (UBTF), CX-5461 that inhibits RPI transcription, and BMH-21 that induces transcription coupled RPI degradation [7,9-12]. However, many other anti-cancer drugs, including Actinomycin D, 5-Fluorouracil, Camptothecin, Bleomycin and others, cause disruption of the nucleolus, the site of ribosome biogenesis [13]. Given that ribosome biogenesis is increasingly recognized as a key target of anticancer drugs and of tumor suppressors [14,15], it is becoming ever more important to understand the underlying molecular mechanisms of their actions.

Some years ago, the p14/p19^{ARF} (ARF) tumor suppressor was shown to inhibit rRNA synthesis and processing in human and mouse [16]. ARF is best documented for its ability to stabilize p53 by inhibiting the MDM2 ubiquitin ligase and in this way to cause cell cycle arrest [17-19]. Initial studies of ARF tumor suppressor function were compounded by the complex overlap between the INK4A and ARF genes [20], but mouse models of ARF-loss [21,22], and ARF inactivation in human cancers [23,24], have clearly identified it as a distinct tumor suppressor. ARF has been implicated as a tumor suppressor in several regulatory pathways, including mitotic checkpoint fidelity and Ras transformation, but in exceptional cases has been shown to also enhance tumorigenesis [25-29]. Inhibition of rRNA synthesis by ARF was proposed to occur via an interaction with nucleophosmin 1 (NPM1, B23), a highly abundant nucleolar chaperone [16,30]. We subsequently demonstrated that in fact ARF interacted directly with Transcription Termination Factor 1 (TTF1, TTF-I) to regulate ribosome biogenesis [31,32]. TTF1 is an essential protein responsible for terminating RPI transcription of the rRNA genes (rDNA). It has also been implicated in rDNA activation [33] and silencing [34], and in polar arrest of rDNA replication [35]. Transport of TTF1 into the nucleolus was shown to depend on NPM1, but to be counteracted by ARF [31,32]. Accumulation of ARF after oncogenic stress was shown to deplete nucleolar TTF1, probably by masking its nucleolar localization signal (NoLS), leading to the inhibition of rRNA synthesis and processing. Here we have mapped the functional NoLS motifs of TTF1 as well as the sequences responsible for ARF-TTF1 interaction. We find that both NoLS sequences and sequences responsible for ARF interaction are distinct but that both lie within semi-redundant 25 amino acid (a.a.) polypeptide repeats present in the N-terminal domain of TTF1.

MATERIALS AND METHODS

Plasmid constructs. Full-length p19^{ARF} (mARF) a.a. 1-169 was obtained from C. J. Sherr. It was sub-cloned and truncated mutants generated in pGEX-4T (Amersham Biosciences) for bacterial expression and sub-cloned as N-terminal HA tagged form into pcDNA3 (Invitrogen). N-terminal FLAG or YFP tagged mouse TTF-I (mTTF1) and mutants were generated by sub-cloning the cDNA open reading frame (NP_033468.2) either into pFLAG-CMV2 (Invitrogen) or pEYFP-C1 (Clontech). Loss of specific DNA binding caused by the W714K mutation of mTTF1 was tested by gel-shift as previously described [36] using bacterially expressed mutant and wild type mTTF a.a.445-859. Note; W714 (NP_033468.2) is equivalent to W688 in the original mTTF1 sequence (NP_033468.1) [36], which lacked one N-terminal repeat.

Antibodies. Antibodies were obtained commercially as follows: anti-FLAG (F7425, Sigma-Aldrich), anti-fibrillarin (MMS-581S, Covance), anti-HA (ab9134, Abcam), anti-YFP (632460, Clontech), anti-HisTag (US Biological).

Cell lines. NIH3T3 and HEK293T were obtained from ATCC and maintained in high glucose Dulbecco's Modified Eagle's Medium (DMEM) supplemented with 10% fetal bovine serum (FBS), penicillin/streptomycin (Wisent), and 2 mM L-glutamine (Wisent).

Transfection. 1.25 x 10^6 HEK293T cells were seeded on poly-L-lysine (1mg/ml) (Sigma) treated 60mm petri dishes 24 hours prior to transfection. For transfections, 1 to 5 ug of total plasmid DNA was diluted in 400µl of Opti-MEM medium (Invitrogen) followed by addition of PEI 2mg/ml (PEI) (Sigma 408727) to obtain a 1:2 DNA:PEI ratio [37-39]. After a 10sec vortex, the mixture is added dropwise to the cells. NIH3T3 cells were plated at 1.5 to 2.5 x 10^5 cells per dish in untreated 3.5cm petri dishes and transfected with 2 to 4 ug total plasmid DNA using jetPRIME (Polyplus) following the manufacturers procedure.

Co-immunoprecipitation was performed as previously described [32]. Briefly, cells were scraped into immunoprecipitations (IP) buffer (25mM Tris-HCl, pH 7.5, 1mM EDTA, 0.1mM EGTA, 5mM $MgCl_2$, 150mM NaCl, 10% glycerol, 1% NP-40 (Igepal, Sigma-Aldrich), 0.1% SDS, 1% TritonX100, and 1µg/ml each pepstatin, leupeptin, and aprotinin (Sigma-Aldrich)), kept on ice for

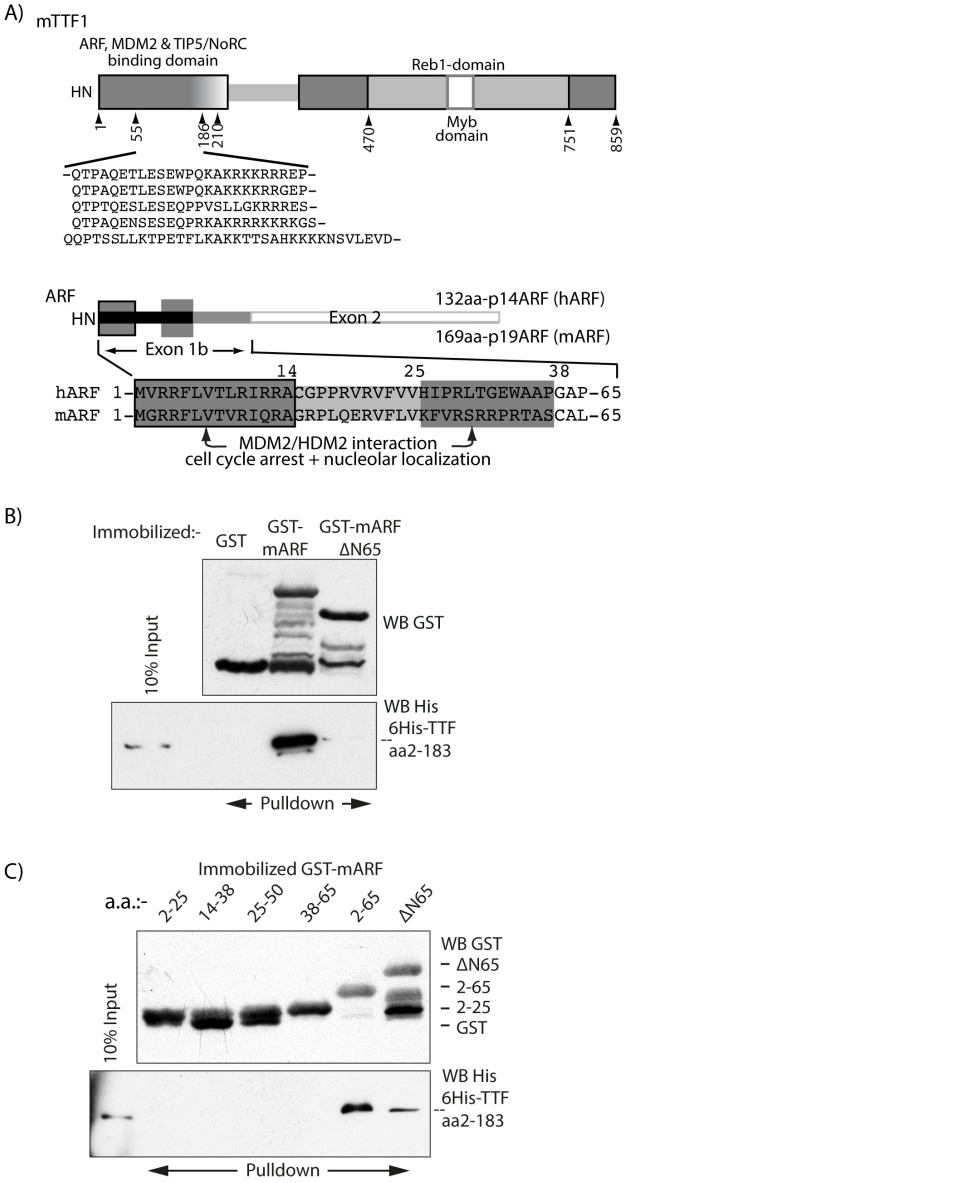

Figure 1. The interaction of the ARF tumor suppressor with the N-terminal domain of mouse (m) TTF1 occurs predominantly via the a.a. 2 to 65 that are semi-conserved between mouse and human. **A**) Diagrammatic structures of mTTF1 and ARF show the Reb1 and Myb homology DNA binding domain, the N-terminal ARF, MDM2 and TIP5/NoRC interaction domain encompassing the 25 a.a. direct sequence repeats of mTTF1 and the mouse-human exon 1b homology domain of ARF and the mapped MDM2/HDM2 interaction domain. **B**) and **C**) GST pull-down interaction assays to determine the mTTF1 binding domain on mARF. GST fusion constructs of full-length and truncation mutants of mARF (GST-mARF (a.a. 1-169), -ΔN65 (a.a. 66-169) and the indicated a.a. ranges) and histidine 6His-tagged mTTF1 a.a. 2-183 (6His-TTF aa2-183) were expressed in E. coli and isolated by affinity chromatography. WB GST and WB His indicate antibodies used in Western blots to detect the immobilized proteins and those pulled-down.

15 min and then sonicated 4 x 20 sec (S-450 Branson Ultrasonics) at maximum power. Cell lysates were cleared, 14,000rpm, 1 min, and incubated with first antibody for 3 hours at 4˚C. 20µg of anti-HA (12CA5) and 20µl of a 1:1 slurry of Protein A-Sepharose (GE Healthcare), or 20µl of anti-FLAG Agarose beads (Sigma) were added to whole cell lysates and incubated at 4°C for 2 hours. Bound proteins were eluted with 2 x SDS-PAGE loading buffer, fractionated on Tris-glycine SDS-PAGE gels, transferred to Nitrocellulose membrane (Bio-Rad) and probed with the appropriate antibodies.

Pull-down assays. Bacterially expressed GST, or GST-ARF fusion constructs were immobilized on G-Sepharose (GE Healthcare) and incubated with cell lysates

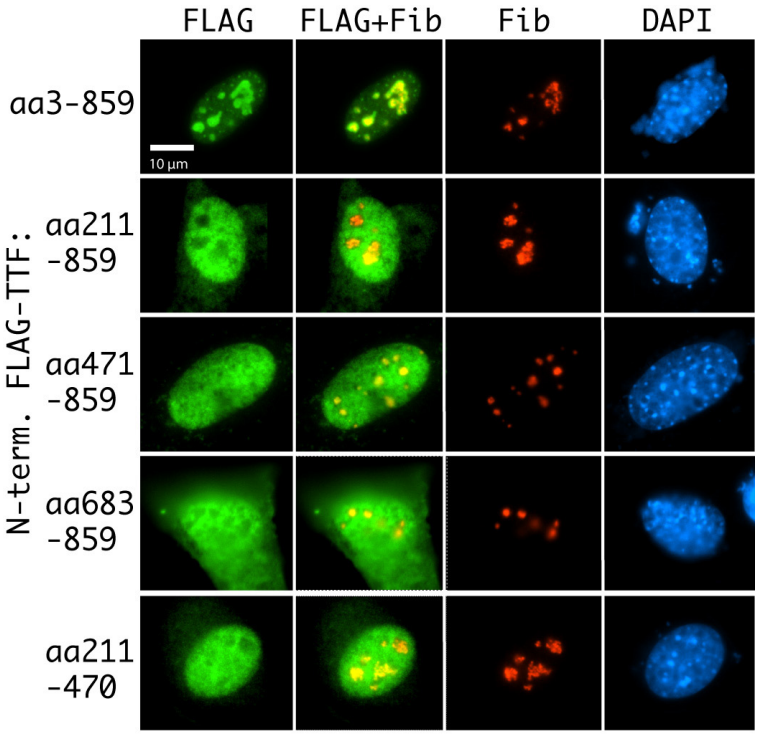

Figure 2. Nucleolar localization of mTTF1 requires a.a. 3-210. FLAG-tagged mTTF1 truncation constructs were expressed in NIH3T3 cells and their nucleolar localization determined by immunofluorescence labelling of the mTTF epitope tag (FLAG) in comparison with endogenous fibrillarin (Fib). FLAG+Fib indicates overlay of the FLAG and fibrillarin images and DAPI indicates DNA staining to reveal the cell nucleus.

prepared from HEK293T cells expressing 6His-TTF1 a.a. 1-183 prepared as for co-immunoprecipitation. The G-Sepharose was then washed five times with NP40 lysis buffer and eluted proteins resolved on SDS–PAGE. After electrophoretic transfer the proteins were revealed by Ponceau Red staining followed by Western Blot using anti-GST antibody (Sigma) and anti-His-Tag antibody (Techniscience).

Immunofluorescence microscopy. For immunofluorescence, cells were fixed with 4% paraformaldehyde/PBS for 15 min, permeabilized with 0.5% Triton/PBS for 5 min, incubated with primary antibodies, either anti-FLAG or anti-YFP, and anti-fibrillarin in 5% goat serum/PBS for 1 hour at RT, stained with anti-rabbit/mouse IgG AlexaFluor 488/568 (Molecular Probes) and then counter-stained with DAPI. After mounting in 50% glycerol/50% 0.2M Na-glycine, 0.3M NaCl, epifluorescent images were generated using a Leica DMI6000 B and OpenLab and Volocity software (Perkin-Elmer Improvision). Where indicated the degree of nucleolar localization was calculated as the ratio of mean nucleolar to nucleoplasmic immunofluorescence signal intensity, FLAG or YFP, using the Volocity (Quorum Technologies Inc.). In each image the DAPI signal was used to delimit the nucleus and the fibrillarin signal the nucleolus, which was excluded when estimating the nuclear YFP signal.

RESULTS

ARF Binds TTF1 via its Conserved MDM2 Interaction Domain

Previous studies had mapped an interaction between ARF and TTF1 to the N-terminal repeats of TTF1 both *in vitro* and *in vivo* [32]. However, the site of this interaction within ARF was not identified. *In vitro* pull-down reactions using an immobilized bacterially expressed GST-mARF fusion confirmed the interaction with N-terminal a.a. 2-183 6xHis-tagged polypeptide of TTF1 expressed in HEK293T, (Figure 1B). Deletion of the first 65 a.a. of mARF, constituting the full mouse-human homology, eliminated or greatly reduced this interaction (Figure 1A, B, and C). In contrast, the N-terminal TTF polypeptide interacted strongly with immobilized mARF a.a. 2-65 but not with subfragments of mARF covering one or other of its MDM2 interaction domains (Figure 1C).

The Nucleolar Localization Signal of TTF1 Maps to the N-terminal Repeat Domain

Both mARF and mTTF1 are considered nucleolar proteins, though they also shuttle between nucleolus and nucleoplasm. A Nucleolar Localization Signal (NoLS) was previously mapped to the N-terminal region of TTF1

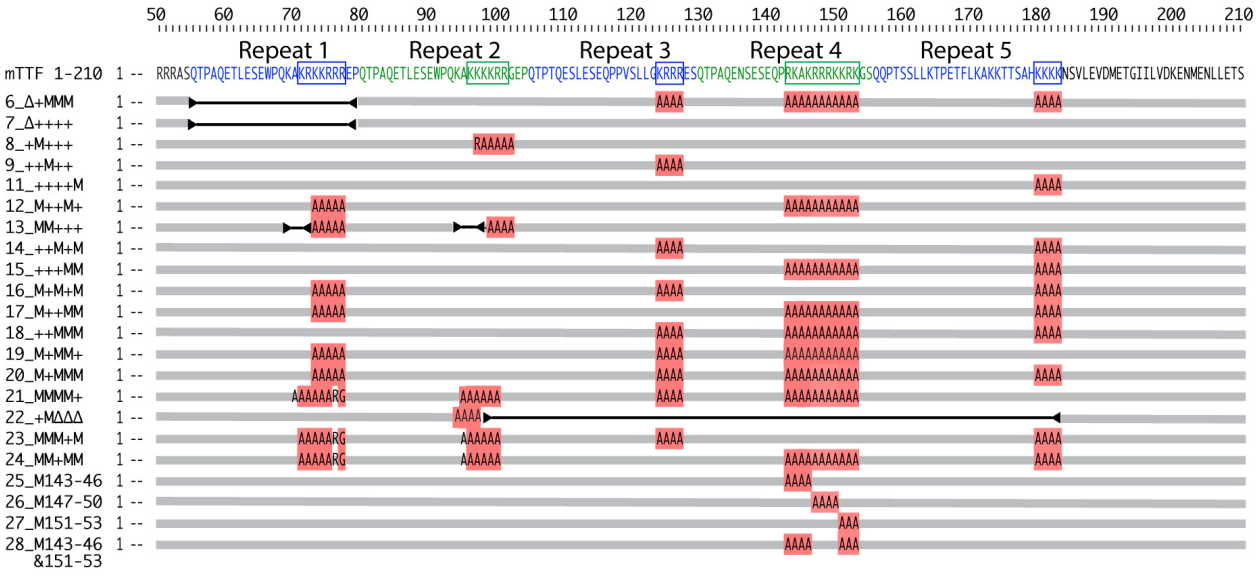

Figure 3. Protein sequence of the YFP-mTTF1 a.a. 2-210 wild type and mutant constructs used to map the sites of nucleolar localization signals (NoLS) and of mARF interactions. The alanine scanning mutations are indicated, as are the deleted sequences (>--<) and mutants are identified by a construct number and a code (e.g. Δ+MMM) indicating which N-terminal repeats were affected in each mutant (Δ = deleted, + = wild type and M = mutated).

[32]. Consistent with this finding, full-length FLAG-tagged TTF1 localized to the nucleolus when expressed in NIH3T3 cells, while deletion of the first 211 amino acids prevented this localization (Figure 2). Neither the N-terminal deletion of TTF1 to a.a. 471 nor to a.a. 683, or expression of the internal a.a. 211 to 470 poly-peptide revealed any other NoLS activity within the rest of the protein.

Multiple Basic Motifs Combine to Create a Strong Autonomous NoLS

Autonomous NoLS motifs are generally rich in basic amino acids [40], and the N-terminal domain of TTF1 contained several such sequences (Figure 3). Indeed, each of the semi-conserved N-terminal repeats contained a run of basic amino acids constituting a potential NoLS (boxed in Figure 3). When the N-terminal polypeptide spanning a.a. 2-210 was tagged N-terminally with YFP and expressed in the NIH3T3 mouse embryonic fibroblast (MEF) cell line, the tag clearly localized to the nucleolus, in agreement with previous data [32]. Each potential NoLS was then deleted or mutated to alanine (A), either singly or in various combinations, and the effect on nucleolar localization determined in NIH3T3 (Figures 3 and 4). Dependent on the mutation, localization of the YFP tag ranged from strongly nucleolar to uniformly nuclear, and some constructs were even excluded from the nucleolus. Individual mutation of repeats 1, 2, 3, and 5 (Figure 4, constructs 7-11) had little or no effect on nucleolar localization. In contrast, combined mutation of repeats 1 and 4 or repeats 3, 4, and 5 (Figure 4, constructs 12 and 18) resulted in uniform YFP distribution throughout the nucleus, while mutation of all potential NoLS motifs but those in repeat 1, 2, or 3 (Figure 4, constructs 22, 6 & 20, and 24), or combined mutation of repeat motifs 1, 4, and 5 or 1, 3, and 4 (Figure 4, constructs 17 and 19), caused significant nucleolar exclusion. This all pointed to the repeat 4 motif as a dominant NoLS, and indeed mutation of all repeat motifs but that of repeat 4 permitted a significant level of nucleolar localization (Figure 4, construct 23). However, localization due to the repeat 4 motif was clearly enhanced by the presence of the repeat 2 motif (Figure 4, constructs 14 and 16). Furthermore, a degree of nucleolar localization could still occur in the absence of the repeat 4 motif (Figure 4 construct 15).

These data suggested that the basic motif in repeat 4 represented a dominant and autonomously functional NoLS, but that its combination with the repeat 2 basic motif generated a much stronger NoLS that functioned at near wildtype levels in targeting the YFP tag to the nucleolus. This said, the basic motifs of repeats 1 to 3 could cooperate to generate a functional NoLS equivalent to that of repeat 4. Consistent with this, repeat 4 contained the longest basic motif with 5 R and 5 K residues, while the next largest motifs were in repeats 1 and 2, respectively of 7 and 6 basic residues (Figure 3). Thus, NoLS strengths of the individual repeats were closely related to the lengths of the contiguous basic motifs they contained. In this context, it was striking that even the YFP-TTF 2-210 constructs lacking NoLS activity were still strongly nuclear, while the YFP moiety alone was not (Figure 4).

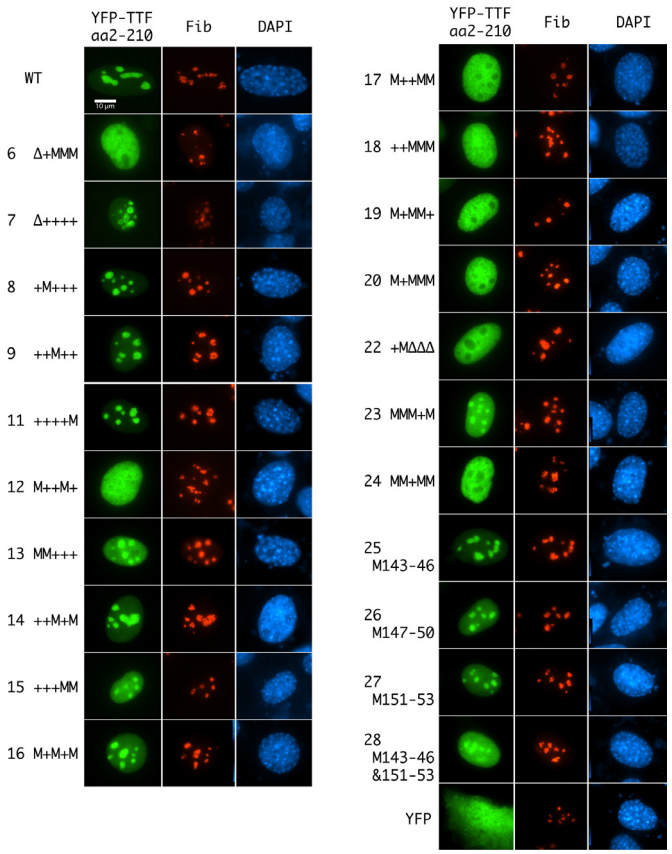

Figure 4. The N-terminal repeats of mTTF1 contain partially redundant nucleolar localization signals (NoLS). N-terminally YFP-fused mTTF1 a.a. 2-210 (YFP-TTF aa2-210) mutant constructs listed in Figure 3 or the unfused YFP construct were expressed in NIH3T3 cells and their nucleolar localization determined by immunofluorescence labelling of the YFP moiety in comparison with endogenous fibrillarin (Fib). DAPI indicates DNA staining used to reveal the extent of the cell nucleus.

This suggested that the basic motifs remaining in these constructs were sufficient for nuclear localization, and hence that nuclear versus nucleolar localization might simply be a function of the length or combined "strength" of these motifs.

To better understand the correlation between the NoLS activity of the dominant N-terminal repeat and its basic motif, contiguous segments of this motif were individually mutated in the context of the YFP-TTF a.a. 2-210 construct, (Figures 3 and 4, constructs 25 to 28). Mutation of any 3 or 4 contiguous lysines/arginines had little effect of nucleolar localization of the construct, while combined deletion of the first 4 and last 3 lysines/arginines strongly reduced but did not eliminate nucleolar localization. This underlines the importance of the length of a basic motif to its NoLS activity.

Interaction Between ARF and TTF1 Depends on Nucleolar Localization

We showed in Figure 1 that the interaction between ARF and TTF1 is mediated by the conserved N-terminal domain of ARF and the N-terminal domain of TTF1. Previously, we had also identified a.a. 121-210 of TTF1 as a minimal region of interaction for ARF and had shown that this region contained a functional NoLS [32]. Our data now show that this same region actually contains the dominant NoLS of N-terminal repeat 4 (Figures 3 and 4). But, to better understand what determines the ARF-TTF interaction we co-expressed mARF with the set of YFP-TTF1 mutant constructs. As expected, mARF coimmunoprecipitated efficiently with the YFP-TTF1 a.a. 2-210 construct, but not with the a.a. 211-470 and only very poorly with a.a. 471-859 constructs. Among the 22 basic motif mutant constructs, ARF interaction corresponded, with few exceptions, with NoLS function (Figure 4 and Table 1). Given that ARF is itself a relatively basic protein (pI of 12.7) and the conserved domain contains 16 basic but only three acidic residues, it is unlikely that the basic motifs within the N-terminal repeats of TTF1 played a direct role in ARF-TTF protein-protein interaction. Thus, the levels of interaction observed in Figure 5

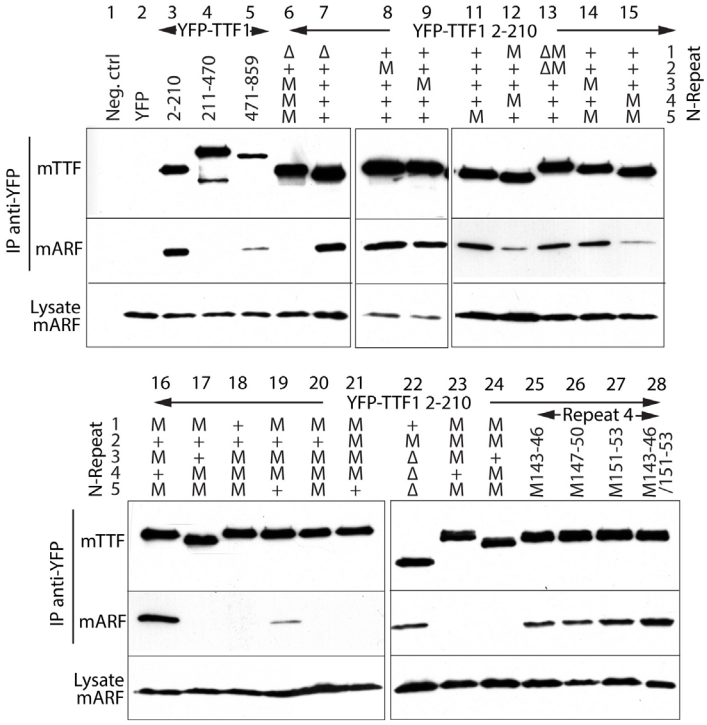

Figure 5. The ARF-TTF1 interaction predominantly depends on TTF1 nucleolar localization. The YFP-fused mTTF1 truncation and alanine scanning mutants used in Figures 2 and 4 were co-expressed with N-terminally HA-tagged full-length mARF in HEK293T cells, total cell lysates prepared and complexes immunoprecipitated via the YFP moiety. The immunoprecipitates were then analyzed by Western blot using anti-YFP and anti-HA antibodies respectively for YFP-TTF1 and HA-mARF in comparison with the total cell lysate. Constructs are indicated as in Figures 2 to 4.

appeared to be driven predominantly by the concentration of each component in the nucleolus. An exception to this was construct 22 that was to some extent excluded from the nucleolus but still interacted moderately well with ARF. However, this construct harbored a large deletion covering N-terminal repeats 3, 4, and 5 which may have revealed a particularly strong interaction domain (Figure 3).

The DNA Binding Domain of TTF1 Plays a Role in its Nucleolar Localization

We had shown that TTF1 lacking the N-terminal domain did not localize to the nucleolus (Figure 2), suggesting that its DNA binding domain did not play a significant role in nucleolar retention. However, to thoroughly test this we also investigated whether the W714K point mutation in the SKWTE motif of the Myb domain known to inactivate DNA binding by TTF1 [36] would affect nucleolar localization. This mutation reduced the degree of nucleolar localization of full-length TTF1 by half as measured by the change in Nucleolar FLAG-TTF / Nucleoplasmic FLAG-TTF ratios from 2.9±0.2 for wild type TTF1 to 1.4±0.1 for the W714K mutant (Figure 6A). When combined with mutation of all 5 N-terminal basic motifs, the W714K nutation led to near complete nucleolar exclusion (Figure 6A, see also Figure 3). DNA binding by TTF1 then enhances its nucleolar localization most probably by slowing release from the nucleolus.

A Single N-terminal Repeat is Sufficient for Nucleolar Localization of TTF1

The data of Figure 4 and 5 suggested that the short sequence repeats within the N-terminal domain of TTF1 functioned to some degree cooperatively in determining its nucleolar localization. However, since the N-terminal repeat 4 played a dominant role, we wished to determine whether this repeat would alone be sufficient to determine nucleolar localization of TTF1. We found that a single copy of repeat 4 was very effective at localizing TTF1 to the nucleolus, when fused to the N-terminally truncated protein, while addition of two copies of the same repeat did not further improve localization and may have generated ectopic nuclear sites (Figure 6B). This leaves open the question of why TTF1 carries multiple N-terminal repeats all with some degree of NoLS activity. These repeats clearly have multiple functions including ARF and

Table 1. Summary of nucleolar localization and mARF interaction for YFP-mTTF a.a. 2-210 wild type and mutant constructs as observed in immunofluorescence and co-immunoprecipitation studies (Figures 3, 4, and 5). The constructs are indicated by number and code (*e.g.* ∆+MMM) indicating which N-terminal repeats are affected in each mutant. An estimate of the degree of nucleolar localization and of ARF interaction for each construct is given from "+++" indicating wild type to "---" indicating none observed.

#	Mutant	Functional NoLS	ARF interacting
	Wild Type	+++	+++
6	∆+MMM	---	---
7	∆++++	++-	+++
8	+M+++	+++	+++
9	++M++	+++	+++
11	++++M	+++	+++
12	M++M+	±--	±--
13	MM+++	++±	++-
14	++M+M	+++	++-
15	+++MM	++-	±--
16	M+M+M	+++	+++
17	M++MM	---	---
18	++MMM	---	---
19	M+MM+	---	±--
20	M+MMM	---	---
21	MMMM+	N/D	---
22	+M∆∆∆	---	++-
23	MMM+M	++-	---
24	MM+MM	---	---
25	M143-46	++±	++-
26	M147-50	++±	++-
27	M151-53	++±	++-
28	M143-46 & 151-53	++±	++-

RNA binding [32,34], and these functions are probably distinct from NoLS activity. By duplicating the repeat with the dominant NoLS we may have disbalanced these different functions. It is interesting, however, to note that the human TTF1 ortholog also carries multiple N-terminal repeats with NoLS-like basic motifs (Figure 6C).

ARF Interaction Site within a Single N-terminal Repeat

The data had shown that the interaction between ARF and TTF1 was dependent on the concentration of TTF1 within the nucleolus. However, the conserved domain of ARF has isoelectric point (pI) in excess of 12, containing 16 basic, but only three acidic residues. Hence, it was unlikely that its direct interaction with the N-terminal repeats of TTF1 was mediated by the basic NoLS motifs. To investigate this interaction further, a single copy of TTF1 N-terminal repeat 4 was fused to YFP and subjected to alanine scanning. Again here, we found that just a single copy of repeat 4 was sufficient for nucleolar localization of YFP (Figure 7A). Mutation of the first 15 amino acids of repeat 4 in groups of five had little effect on this nucleolar localization, while mutation of either NoLS-associated basic motifs KAKKR and more so RKKRK reduced but did not eliminate nucleolar localization. Each construct was then co-expressed with mARF and interactions analyzed by co-immunoprecipitation. The wild type YFP-Repeat 4 construct interacted significantly with ARF, while mutation of the NoLS associated sequences reduced or eliminated this interaction qualitatively consistent with the effect on nucleolar localization. In contrast, mutation of the central Repeat 4 sequences ENSES and more especially EQPR greatly reduced the interaction but did not affect nucleolar localization (Figure 7B). Interestingly, these latter two motifs contain the only three acidic residues of repeat 4 and these residues

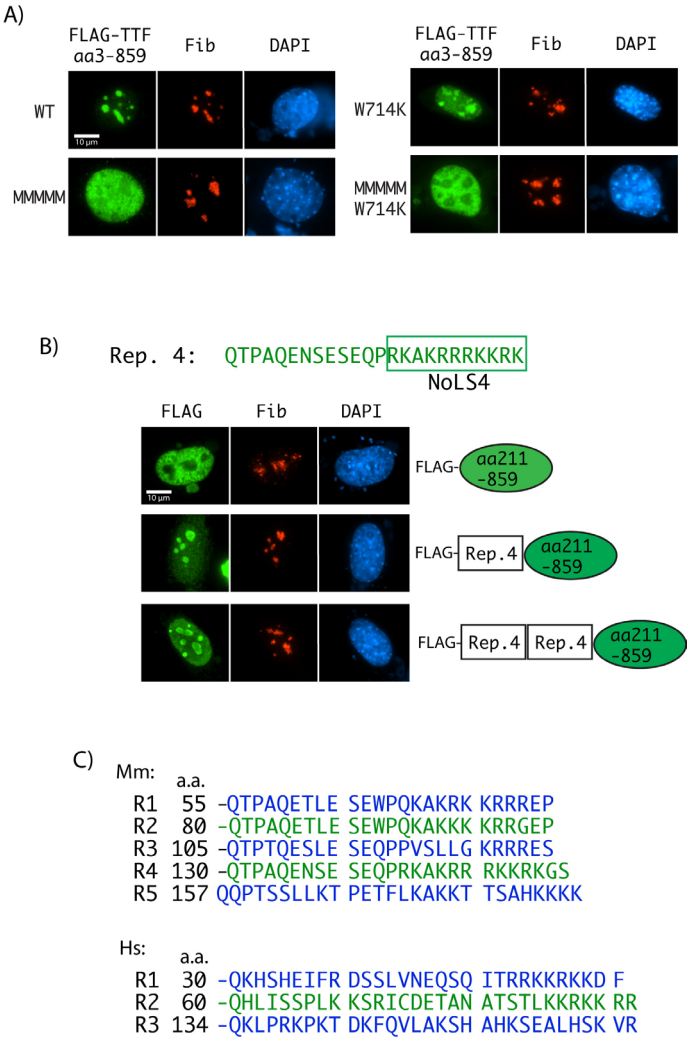

Figure 6. The DNA binding domain plays a minor role in nucleolar localization of mTTF1. A) FLAG-tagged mTTF1 constructs either wild type (WT) or carrying K/R to A mutations in all basic motifs of the five N-terminal repeats (as Figure 3) were expressed in NIH3T3 cells in parallel with these same constructs carrying the W714K in order to inactivate their DNA sequence specific binding. Nucleolar localization was determined by immunofluorescence labelling of the mTTF epitope tag (FLAG) in comparison with endogenous fibrillarin (Fib). DAPI indicates DNA staining used to reveal the cell nucleus. B) One or two copies of N-terminal repeat 4 were fused to a.a. 211-859 of mTTF1 and expressed in a FLAG-tagged form in NIH3T3 cells in parallel with truncated mTTF1 a.a. 211-859. Nucleolar localization was then revealed as in A). C) Comparison of the N-terminal sequences of mouse (Mm) and human (Hs) TTF1 reveal three partial repeats containing likely NoLS motifs in human TTF1 (NP_031370.2).

are conserved in repeats 1 to 4 (Figure 6C), suggesting they might play a part in forming salt bridges with the many basic residues of ARF.

DISCUSSION

Before the present study little was known of the substructure of the N-terminal repeat domain of TTF1, despite several functions having been ascribed to this domain including regulation of sequence specific DNA binding [36,41], recruitment of chromatin remodeling and silencing complexes such as NoRC either directly [42] or via non-coding RNA [34], and recruitment of the ARF tumor suppressor [31,32]. Our data show that the interaction of TTF with ARF is driven by a combination of factors, but predominant among these is the degree of nucleolar localization of these proteins. Localization of TTF1 was previously shown to be highly dynamic, the factor shuttling rapidly between nucleoplasm and nucleolus [32]. Here we show that its nucleolar localization depends predominantly on the NoLS activity of the N-terminal repeats and to a lesser extent on sequence-specific DNA binding via the Reb1/Myb domain that presumably plays a role in nucleolar retention. We further show that

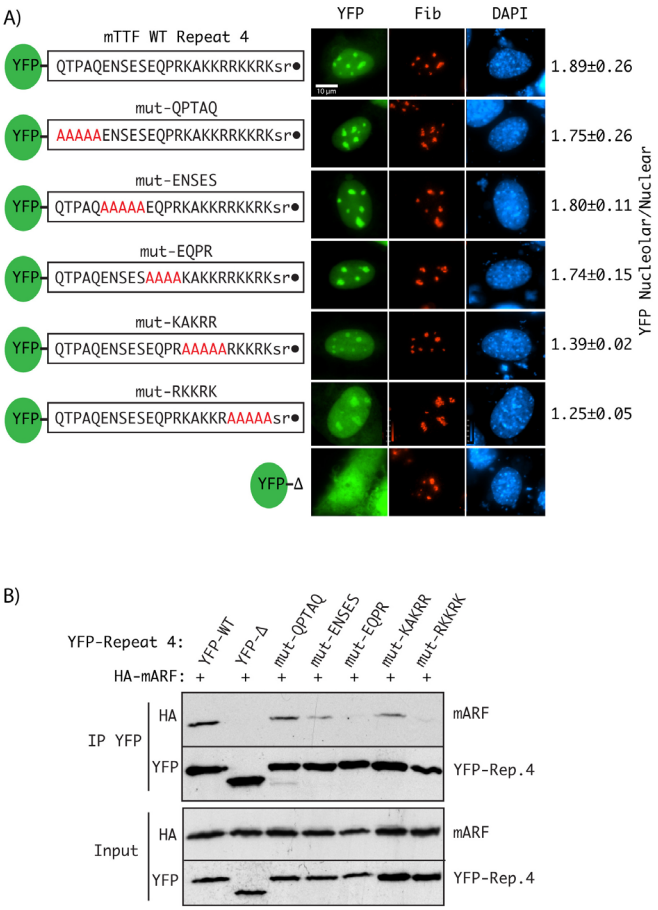

Figure 7. The interaction of mTTF1 with ARF also depends on sequences adjacent to the NoLS motif of the N-terminal repeats. A) A single copy of mTTF1 N-terminal repeat 4 was fused C-terminally to a YFP moiety and the construct subjected to alanine scanning mutation. After expression in NIH3T3 cells, nucleolar localization of YFP was determined in parallel with endogenous fibrillarin (Fib) by immunofluorescent labelling using anti-YFP and anti-fibrillarin antibodies. DAPI indicates DNA staining to reveal the cell nucleus. The ratio of nucleolar to nucleoplasmic YFP is indicated (YFP Nucleolar/Nuclear), see Materials and Methods. B) The same series of YFP-fusion constructs as in A) were co-expressed with HA-mARF in HEK293T cells and proteins immunoprecipitating with the YFP moiety analyzed by Western blot using anti-YFP (IP YFP) and anti-HA antibodies in comparison with total cell lysates (Input).

these repeats are responsible for a direct interaction with the N-terminal conserved domain of ARF that regulates Mdm2 activity and cell cycle arrest. This provides important molecular detail in support of our previous observation that ARF can regulate the nucleolar localization of TTF1 by regulating its NoLS activity and in this way suppress ribosome biogenesis [32].

Our data show that TTF1 nucleolar localization is driven by the cooperative effect of basic NoLS motifs contained within all five of the N-terminal repeats, but that motif 4 contains a semi-dominant NoLS. A similar cooperative scenario seems likely for the interaction of these same repeats with ARF, but this was not directly tested. The sequences of both the ARF conserved domain and the relatively proline-rich N-terminal domain of TTF1 suggest that they exist in relatively unstructured and extended forms [43]. In the case of TTF1, this most likely explains the ability of the N-terminal domain to inhibit DNA binding by the Reb/Myb domain via an intramolecular interaction. However, the NoLS motifs would be unlikely to be involved in such an intramolecular interaction due to their strong positive charge. A similar argument can be made for the interaction with ARF, which has a pI in excess of 12. Mutation analysis of the interaction of the dominant N-terminal TTF repeat 4 with ARF supports this contention and suggests that the interaction requires motifs central to the repeat and conserved in four of the five repeats. It is also suggested that the three acidic residues in these conserved motifs could play a part by forming salt linkages with the many arginines in ARF.

Acknowledgments: This work was funded by operating grants from the Canadian Institutes of Health Research (CIHR, MOP12205/PJT153266) and the National Science and Engineering Council (NSERC) of Canada. The Research Centre of the Québec University Hospital Centre (CHU de Québec) is supported by the Fonds de Recherche du Québec - Santé (FRQS).

REFERENCES

1. Hooper ML. Tumour suppressor gene mutations in humans and mice: parallels and contrasts. EMBO J. 1998 Dec;17(23):6783–9.
2. Kastenhuber ER, Lowe SW. Putting p53 in Context. Cell. 2017 Sep;170(6):1062–78.
3. Penzo M, Montanaro L, Treré D, Derenzini M. The Ribosome Biogenesis-Cancer Connection. Cells. 2019 Jan;8(1):E55.
4. Aspesi A, Ellis SR. Rare ribosomopathies: insights into mechanisms of cancer. Nat Rev Cancer. 2019 Apr;19(4):228–38.
5. Pelletier J, Thomas G, Volarević S. Ribosome biogenesis in cancer: new players and therapeutic avenues. Nat Rev Cancer. 2018 Jan;18(1):51–63.
6. Núñez Villacís L, Wong MS, Ferguson LL, Hein N, George AJ, Hannan KM. New Roles for the Nucleolus in Health and Disease. BioEssays. 2018 May;40(5):e1700233.
7. Hamdane N, Herdman C, Mars JC, Stefanovsky V, Tremblay MG, Moss T. Depletion of the cisplatin targeted HMGB-box factor UBF selectively induces p53-independent apoptotic death in transformed cells. Oncotarget. 2015 Sep;6(29):27519–36.
8. Hamdane N, Stefanovsky VY, Tremblay MG, Németh A, Paquet E, Lessard F, et al. Conditional inactivation of Upstream Binding Factor reveals its epigenetic functions and the existence of a somatic nucleolar precursor body. PLoS Genet. 2014 Aug;10(8):e1004505.
9. Bywater MJ, Poortinga G, Sanij E, Hein N, Peck A, Cullinane C, et al. Inhibition of RNA polymerase I as a therapeutic strategy to promote cancer-specific activation of p53. Cancer Cell. 2012 Jul;22(1):51–65.
10. Drygin D, Lin A, Bliesath J, Ho CB, O'Brien SE, Proffitt C, et al. Targeting RNA Polymerase I with an Oral Small Molecule CX-5461 Inhibits Ribosomal RNA Synthesis and Solid Tumor Growth. Cancer Res. 2011 Feb 15;71(4):1418-30. doi: 10.1158/0008-5472.CAN-10-172.
11. Peltonen K, Colis L, Liu H, Jäämaa S, Zhang Z, Af Hällström T, et al. Small molecule BMH-compounds that inhibit RNA polymerase I and cause nucleolar stress. Mol Cancer Ther. 2014 Nov;13(11):2537–46.
12. Colis L, Peltonen K, Sirajuddin P, Liu H, Sanders S, Ernst G, et al. DNA intercalator BMH-21 inhibits RNA polymerase I independent of DNA damage response. Oncotarget. 2014 Jun;5(12):4361–9.
13. Rubbi CP, Milner J. Disruption of the nucleolus mediates stabilization of p53 in response to DNA damage and other stresses. EMBO J. 2003 Nov;22(22):6068–77.
14. Quin JE, Devlin JR, Cameron D, Hannan KM, Pearson RB, Hannan RD. Targeting the nucleolus for cancer intervention. Biochim Biophys Acta. 2014 Jun;1842(6):802–16.
15. Bustelo XR, Dosil M. Ribosome biogenesis and cancer: basic and translational challenges. Curr Opin Genet Dev. 2018 Feb;48:22–9.
16. Sugimoto M, Kuo ML, Roussel MF, Sherr CJ. Nucleolar Arf tumor suppressor inhibits ribosomal RNA processing. Mol Cell. 2003 Feb;11(2):415–24.
17. Bothner B, Lewis WS, DiGiammarino EL, Weber JD, Bothner SJ, Kriwacki RW. Defining the molecular basis of Arf and Hdm2 interactions. J Mol Biol. 2001 Nov;314(2):263–77.
18. Weber JD, Jeffers JR, Rehg JE, Randle DH, Lozano G, Roussel MF, et al. p53-independent functions of the p19(ARF) tumor suppressor. Genes Dev. 2000 Sep;14(18):2358–65.
19. Sherr CJ, Weber JD. The ARF/p53 pathway. Curr Opin Genet Dev. 2000 Feb;10(1):94–9.
20. Sherr CJ. The INK4a/ARF network in tumour suppression. Nat Rev Mol Cell Biol. 2001 Oct;2(10):731–7.
21. Lowe SW, Sherr CJ. Tumor suppression by Ink4a-Arf: progress and puzzles. Curr Opin Genet Dev. 2003 Feb;13(1):77–83.
22. Sharpless NE, Ramsey MR, Balasubramanian P, Castrillon DH, DePinho RA. The differential impact of p16(INK4a) or p19(ARF) deficiency on cell growth and tumorigenesis. Oncogene. 2004 Jan;23(2):379–85.
23. Williams RT, Sherr CJ. The ARF tumor suppressor in acute leukemias: insights from mouse models of Bcr-Abl-induced acute lymphoblastic leukemia. Adv Exp Med Biol. 2007;604:107–14.
24. Harland M, Taylor CF, Chambers PA, Kukalizch K, Randerson-Moor JA, Gruis NA, et al. A mutation hotspot at the p14ARF splice site. Oncogene. 2005 Jun;24(28):4604–8.
25. El-Athman R, Genov NN, Mazuch J, Zhang K, Yu Y, Fuhr L, et al. The Ink4a/Arf locus operates as a regulator of the circadian clock modulating RAS activity. PLoS Biol. 2017 Dec;15(12):e2002940.
26. Xie Y, Liu S, Lu W, Yang Q, Williams KD, Binhazim AA, et al. Slug regulates E-cadherin repression via p19Arf in prostate tumorigenesis. Mol Oncol. 2014 Oct;8(7):1355–64.
27. Britigan EM, Wan J, Zasadil LM, Ryan SD, Weaver BA. The ARF tumor suppressor prevents chromosomal instability and ensures mitotic checkpoint fidelity through regulation of Aurora B. Mol Biol Cell. 2014 Sep;25(18):2761–73.
28. Chen Z, Carracedo A, Lin HK, Koutcher JA, Behrendt N, Egia A, et al. Differential p53-independent outcomes of p19(Arf) loss in oncogenesis. Sci Signal. 2009 Aug;2(84):ra44.
29. Zhang Y, Saporita AJ, Weber JD. P19ARF and RasV^{12} offer opposing regulation of DHX33 translation to dictate tumor cell fate. Mol Cell Biol. 2013 Apr;33(8):1594–607.
30. Itahana K, Bhat KP, Jin A, Itahana Y, Hawke D, Kobayashi R, et al. Tumor suppressor ARF degrades B23, a nucleolar protein involved in ribosome biogenesis and cell proliferation. Mol Cell. 2003 Nov;12(5):1151–64.
31. Lessard F, Stefanovsky V, Tremblay MG, Moss T. The cellular abundance of the essential transcription termination factor TTF-I regulates ribosome biogenesis and is determined by MDM2 ubiquitinylation. Nucleic Acids Res. 2012 Jul;40(12):5357–67.

32. Lessard F, Morin F, Ivanchuk S, Langlois F, Stefanovsky V, Rutka J, et al. The ARF tumor suppressor controls ribosome biogenesis by regulating the RNA polymerase I transcription factor TTF-I. Mol Cell. 2010 May;38(4):539–50.
33. Németh A, Strohner R, Grummt I, Längst G. The chromatin remodeling complex NoRC and TTF-I cooperate in the regulation of the mammalian rRNA genes in vivo. Nucleic Acids Res. 2004 Aug;32(14):4091–9.
34. Savić N, Bär D, Leone S, Frommel SC, Weber FA, Vollenweider E, et al. lncRNA maturation to initiate heterochromatin formation in the nucleolus is required for exit from pluripotency in ESCs. Cell Stem Cell. 2014 Dec;15(6):720–34.
35. Akamatsu Y, Kobayashi T. The Human RNA Polymerase I Transcription Terminator Complex Acts as a Replication Fork Barrier That Coordinates the Progress of Replication with rRNA Transcription Activity. Mol Cell Biol. 2015 May;35(10):1871–81.
36. Evers R, Smid A, Rudloff U, Lottspeich F, Grummt I. Different domains of the murine RNA polymerase I-specific termination factor mTTF-I serve distinct functions in transcription termination. EMBO J. 1995 Mar;14(6):1248–56.
37. Reed SE, Staley EM, Mayginnes JP, Pintel DJ, Tullis GE. Transfection of mammalian cells using linear polyethylenimine is a simple and effective means of producing recombinant adeno-associated virus vectors. J Virol Methods. 2006 Dec;138(1-2):85–98.
38. Boussif O, Lezoualc'h F, Zanta MA, Mergny MD, Scherman D, Demeneix B, et al. A versatile vector for gene and oligonucleotide transfer into cells in culture and in vivo: polyethylenimine. Proc Natl Acad Sci U S A. 1995 Aug 1;92(16):7297-301.
39. Scott RP, Eketjäll S, Aineskog H, Ibáñez CF. Distinct turnover of alternatively spliced isoforms of the RET kinase receptor mediated by differential recruitment of the Cbl ubiquitin ligase. J Biol Chem. 2005 Apr;280(14):13442–9.
40. Emmott E, Hiscox JA. Nucleolar targeting: the hub of the matter. EMBO Rep. 2009 Mar;10(3):231–8.
41. Sander EE, Mason SW, Munz C, Grummt I. The amino-terminal domain of the transcription termination factor TTF-I causes protein oligomerization and inhibition of DNA binding. Nucleic Acids Res. 1996 Oct;24(19):3677–84.
42. Zhou Y, Santoro R, Grummt I. The chromatin remodeling complex NoRC targets HDAC1 to the ribosomal gene promoter and represses RNA polymerase I transcription. EMBO J. 2002 Sep;21(17):4632–40.
43. DiGiammarino EL, Filippov I, Weber JD, Bothner B, Kriwacki RW. Solution structure of the p53 regulatory domain of the p19Arf tumor suppressor protein. Biochemistry. 2001 Feb;40(8):2379–86.